Design of Reactive Parasitic Elements in Electronic Beam Steering Arrays

Beat Schaer, K. Rambabu, Jens Bornemann, *Fellow, IEEE*, and Rüdiger Vahldieck, *Fellow, IEEE*

***Abstract*—A new approach for the design of electronic beam steering arrays with reactive parasitic elements is introduced. The method is demonstrated at the example of a circular array formed by capacitively tuned monopoles. The related capacitances are determined straightforwardly and without any need for optimization techniques. The resulting beams are rotatable and maintain their gain and beamwidth within tight margins. Comparisons with NEC2 verify the pattern calculation.**

***Index Terms*—Beam steering, circular arrays, parasitic antennas, phased arrays.**

I. Introduction

ELECTRONIC beam steering is frequently used in mobile applications to enhance spectrum efficiency as well as to reduce problems associated with multipath propagation. Recent results in information theory have demonstrated an enormous potential for channel capacity of wireless systems with multiple antennas at both the transmitter and the receiver, e.g., the so-called multiple-input multiple-output (MIMO) systems [1]. Antenna beam forming networks (BFNs) have been mostly implemented by digitally based architectures. The digital beam forming (DBF) architecture [2] offers several functionalities like programmable control of antenna radiation pattern, direction-of-arrival (DOA) estimation and adaptive steering of the transmitting antenna beam to enhance the signal-to-interference-noise ratio (SINR). An unfortunate aspect of these digital architectures is the high cost of employing a radio receiver for each antenna element, thus resulting in relatively high losses in the respected feed circuits.

The analog approach, on the other hand, is re-emerging to create an alternative architecture of adaptive array antennas. The history of practical analog beam-forming antennas dates back to the Butler matrix [3], which consists of hybrids as fixed phase shifters. Since beam steering is operated by employing selective RF switches, the steering angle is only discrete. An alternative approach for beam steering using varactor-tuned passive radiators is proposed in [4]. Compared to the Butler matrix method, the variable beam direction in this approach can have a higher resolution in the beam direction. The proposed beam forming approach utilizes one active and multiple passive radiators. By adding varactors to the passive radiators, beam steering is facilitated by controlling the phases of the currents in the passive radiators. To estimate the value of the capacitances required to focus the beam in a particular direction, optimization techniques are employed [5]. However, optimization schemes have many drawbacks, such as convergence and excess time frames toward a final design.

Manuscript received November 14, 2003; revised November 23, 2004.

B. Schaer was with the Laboratory for Electromagnetic Fields and Microwave Electronics, the Swiss Federal Institute of Technology (ETH) Zürich, Zürich, Switzerland. He is now with the Swiss Broadcasting Corporation, CH-3000 Berne, Switzerland.

K. Rambabu and J. Bornemann are with the Department of Electrical and Computer Engineering, University of Victoria, Victoria, BC V8W 3P6, Canada.

R. Vahldieck is with the Laboratory for Electromagnetic Fields and Microwave Electronics, the Swiss Federal Institute of Technology (ETH) Zürich, Zürich, CH-8092, Switzerland.

Digital Object Identifier 10.1109/TAP.2005.848452

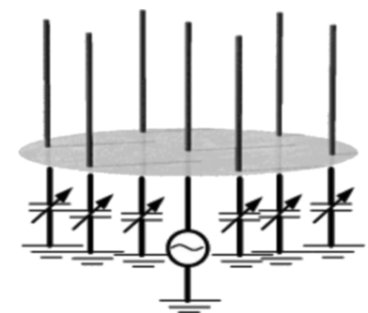

Fig. 1. Basic antenna arrangement consisting of quarter-wavelength monopoles equally spaced at a quarter-wavelength from the center monopole.

Therefore, this paper focuses on an analytical design approach for computing the capacitances required in general arrays using tunable parasitic elements.

II. Formulation

Fig. 1 shows the basic arrangement of the proposed beam-forming scheme with parasitic elements. To demonstrate the proposed technique, we first consider a circular array of six parasitic elements and an active radiator at the center. Each element consists of a quarter-wavelength vertical monopole fixed to a base plate and a variable capacitor. For far-field analysis using image theory, each reactive monopole is treated as a dipole with a center capacitor. The active radiator is connected to a voltage source. The radiators are assumed to be wires of diameter $\mathrm{d} < \lambda/100$ and are located at a radius of $\lambda/4$ around the center element. Assuming for simplicity that the center element is surrounded by six parasitic elements, then the basic antenna arrangement can be represented as a seven-port network as shown in Fig. 2.

Including mutual coupling between the elements, the equation for the center element is represented by

$$V_0 = \sum_{k=0}^{N} Z_{0k}\underline{I}_k \tag{1-a}$$

whereas that for the parasitic elements $(1 \leq i \leq N)$ is

$$-\left(\frac{1}{jwC_i}\right)\underline{I}_i = \sum_{k=0}^{N} Z_{ik}\underline{I}_k \tag{1-b}$$

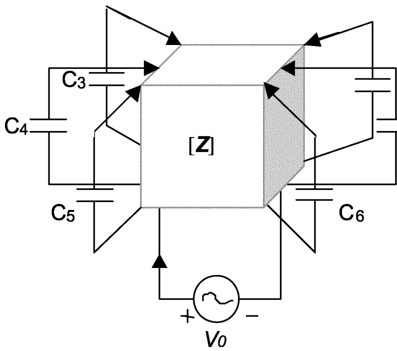

Fig. 2. Seven-port network representing the basic antenna arrangement of Fig. 1.

The electric far field is represented by

$$E(r,\theta,\phi) = EF \cdot \underbrace{\sum_{i=1}^{N} I_i' e^{j\left[kd\sin\theta\cos(\phi-\phi_i)+\alpha_i'\right]}}_{AF(\theta,\phi) \text{ of a circular array}} \tag{2}$$

where EF represents the element factor, ϕ_i denote the angular positions of the elements, and I_i' and α_i' the currents and phases, respectively, obtained from classical circular array theory, e.g., [6]. The array factor is mainly dominated by the dipole currents, which depend on the impedance matrix and the capacitances, as well as on the voltage source of the active dipole.

Based on the fact that the current is a nonlinear function of the reactances and that the capacitances must be realizable ($C_i > 0$), the phase control of the parasitic radiators is crucial. The required phase excitations α_i' of each dipole can be determined by the array factor to direct the main beam in a certain direction. However, the array factor *neglects* mutual coupling.

Therefore, the task is to replace I_i' and α_i' by the actual complex currents $\underline{I}_i$ and, hence, reproduce the array factor *including* the mutual interactions of the elements. Moreover, to maximize the output signal in a desired direction, we will solve for capacitances C_i in an efficient and straightforward way and without any use of lengthy optimization algorithms. In order to achieve this goal, we first represent the complex currents by their amplitudes and phases

$$\underline{I}_i = I_i a_i = I_i e^{j\alpha_i} \tag{3}$$

and rearrange (1), e.g., for $N = 6$ passive elements.

$$\begin{bmatrix} V_0 \\ I_1 a_1\left(j\dfrac{1}{wC_1}\right) \\ I_2 a_2\left(j\dfrac{1}{wC_2}\right) \\ I_3 a_3\left(j\dfrac{1}{wC_3}\right) \\ I_4 a_4\left(j\dfrac{1}{wC_4}\right) \\ I_5 a_5\left(j\dfrac{1}{wC_5}\right) \\ I_6 a_6\left(j\dfrac{1}{wC_6}\right) \end{bmatrix} = \begin{bmatrix} Z_{00} & Z_{01} & Z_{02} & Z_{03} & Z_{04} & Z_{05} & Z_{06} \\ Z_{10} & Z_{11} & Z_{12} & Z_{13} & Z_{14} & Z_{15} & Z_{16} \\ Z_{20} & Z_{21} & Z_{22} & Z_{23} & Z_{24} & Z_{25} & Z_{26} \\ Z_{30} & Z_{31} & Z_{32} & Z_{33} & Z_{34} & Z_{35} & Z_{36} \\ Z_{40} & Z_{41} & Z_{42} & Z_{43} & Z_{44} & Z_{45} & Z_{46} \\ Z_{50} & Z_{51} & Z_{52} & Z_{53} & Z_{54} & Z_{55} & Z_{56} \\ Z_{60} & Z_{61} & Z_{62} & Z_{63} & Z_{64} & Z_{65} & Z_{66} \end{bmatrix} \begin{bmatrix} I_0 a_0 \\ I_1 a_1 \\ I_2 a_2 \\ I_3 a_3 \\ I_4 a_4 \\ I_5 a_5 \\ I_6 a_6 \end{bmatrix} \tag{4}$$

It is obvious that the amplitudes of the passive radiators will be smaller than that of the center active one and that they differ due to the different capacitances at their bases. The current in the active radiator due to the voltage source V_0 and under the influence of mutual coupling can be written as in (5), shown at the bottom of page. Now, the framed part of (4) is rearranged as

$$I_i a_i \left(j\frac{1}{wC_i}\right) = \sum_{k=0}^{N} Z_{ik} I_k a_k. \tag{6}$$

Using the fact that the term in parenthesis is purely imaginary, we write

$$\mathrm{Re}\left[j\frac{1}{wC_i}\right] \stackrel{!}{=} 0 = \mathrm{Re}\left[\frac{1}{I_i a_i}\sum_{k=0}^{N} Z_{ik} I_k a_k\right] \tag{7}$$

and, since $I_1 \in \Re$, we obtain

$$0 = \mathrm{Re}\left[\frac{1}{a_i}\sum_{k=0}^{N} Z_{ik} I_k a_k\right]. \tag{8}$$

Similarly, we arrange all equations within the framed part of (4), as shown in (9) at bottom of the page. By inserting (5) into (9),

$$I_0 a_0 = \frac{V_0 - (I_1 a_1 Z_{01} + I_2 a_2 Z_{02} + I_3 a_3 Z_{03} + I_4 a_4 Z_{04} + I_5 a_5 Z_{05} + I_6 a_6 Z_{06})}{Z_{00}} \tag{5}$$

$$\underbrace{\begin{bmatrix} -\mathrm{Re}\left(\frac{I_0 a_0 Z_{10}}{a_1}\right) \\ -\mathrm{Re}\left(\frac{I_0 a_0 Z_{10}}{a_2}\right) \\ -\mathrm{Re}\left(\frac{I_0 a_0 Z_{10}}{a_3}\right) \\ -\mathrm{Re}\left(\frac{I_0 a_0 Z_{10}}{a_4}\right) \\ -\mathrm{Re}\left(\frac{I_0 a_0 Z_{10}}{a_5}\right) \\ -\mathrm{Re}\left(\frac{I_0 a_0 Z_{10}}{a_6}\right) \end{bmatrix}}_{\boldsymbol{b}} = \underbrace{\begin{bmatrix} \mathrm{Re}\left(\frac{a_1 Z_{11}}{a_1}\right) & \mathrm{Re}\left(\frac{a_2 Z_{12}}{a_1}\right) & \mathrm{Re}\left(\frac{a_3 Z_{13}}{a_1}\right) & \cdots & \cdots & \mathrm{Re}\left(\frac{a_6 Z_{16}}{a_1}\right) \\ \mathrm{Re}\left(\frac{a_1 Z_{21}}{a_2}\right) & \mathrm{Re}\left(\frac{a_2 Z_{22}}{a_2}\right) & & & & \vdots \\ \mathrm{Re}\left(\frac{a_1 Z_{31}}{a_3}\right) & \mathrm{Re}\left(\frac{a_2 Z_{32}}{a_3}\right) & \ddots & & & \vdots \\ \mathrm{Re}\left(\frac{a_1 Z_{41}}{a_4}\right) & \mathrm{Re}\left(\frac{a_2 Z_{42}}{a_4}\right) & & \ddots & & \vdots \\ \mathrm{Re}\left(\frac{a_1 Z_{51}}{a_5}\right) & \mathrm{Re}\left(\frac{a_2 Z_{52}}{a_5}\right) & & & \ddots & \vdots \\ \mathrm{Re}\left(\frac{a_1 Z_{61}}{a_6}\right) & \mathrm{Re}\left(\frac{a_2 Z_{62}}{a_6}\right) & \cdots & \cdots & \cdots & \mathrm{Re}\left(\frac{a_6 Z_{66}}{a_6}\right) \end{bmatrix}}_{\boldsymbol{A}} \underbrace{\begin{bmatrix} I_1 \\ I_2 \\ I_3 \\ I_4 \\ I_5 \\ I_6 \end{bmatrix}}_{\boldsymbol{x}} \tag{9}$$

we obtain vector $\boldsymbol{b}$ as

$$b=-\mathrm{Re}\left\{\left[\frac{V_0Z_{10}}{a_1Z_{00}}\ \frac{V_0Z_{10}}{a_2Z_{00}}\ \frac{V_0Z_{10}}{a_3Z_{00}}\ \frac{V_0Z_{10}}{a_4Z_{00}}\ \frac{V_0Z_{10}}{a_5Z_{00}}\ \frac{V_0Z_{10}}{a_6Z_{00}}\right]^T\right\} \tag{10}$$

vector $\boldsymbol{x}$ follows from (9), and matrix $\boldsymbol{A}$ is shown in (11) at the bottom of the page. By inverting $\boldsymbol{A}$, the amplitudes of the currents are determined and are used to estimate $C_1 \ldots C_6$. However, some of the so-obtained capacitances may be negative due to the fact that for a desired beam direction, the parasitic elements located in that direction act as directors (capacitive) while those in the opposite direction represent reflectors (inductive). In order to make the capacitances realizable $(C_i > 0)$, we use the phase α_0 of the center element to obtain a modified set of capacitances under the condition that the electric field in the specified direction be maximized

$$\max\left|\frac{AF}{e^{j\alpha_0}}\right| = \max\left|I_0 + \sum_{i=1}^{N} I_i e^{j[kd\sin\theta\cos(\phi-\phi_i)+\alpha_i-\alpha_0]}\right|. \tag{12}$$

Note that after the new set of C's is determined, the actual phase of the feeding element is irrelevant for the far-field pattern of the array; in other words, the phases are normalized to that of the feeding element.

III. Results

In order to validate the far-field calculations, the radiation patterns and maximum E-fields of a system with six parasitic elements are presented. The radius of each radiator is assumed to be 0.001λ, and the frequency is 2.484 GHz. The results obtained with our in-house code are compared with those of the Numerical Electromagnetics Code NEC2. Fig. 3 demonstrates that the results are in excellent agreement. The maximum E-fields are calculated as 2.3 V/m (this method) and 2.2 V/m (NEC2).

By solving for the capacitances as outlined in the previous section, the beam can be rotated. Table I shows the various parameters of the patterns obtained for beams positioned at every

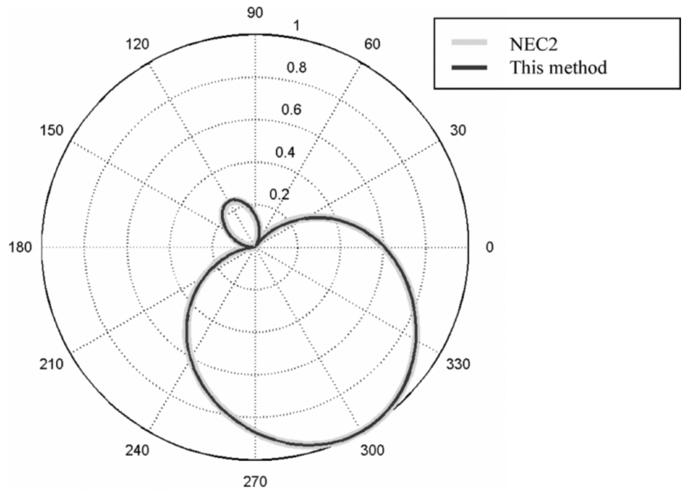

Fig. 3. Principal plane E-field amplitude pattern $(\theta = \pi/2)$ for the beam focused in 300° position.

15° in the azimuth plane. Although a maximum E-field and directivity are only achieved in the exact direction of a parasitic element (multiples of 60° in Table I), the respective E-field values $(\mathrm{E_d}/\mathrm{E_{max}}$ in Table I) drop only very slightly in directions anywhere between the element locations. It has even been demonstrated (not shown here) that on a one-degree resolution and a tolerance level of 0.1 pF for the capacitances, the minimum E-field $\mathrm{E_d}$ in the direction of the beam will never drop below 85 percent of the maximum possible E-field $\mathrm{E_{max}}$.

One of the advantages of this method is the fact that during the calculation of the final set of capacitances, the minimum and maximum realizable capacitances as well as their accuracies can be specified. Table II lists the final values obtained for the directions given in Table I and the following conditions for the capacitances: $\mathrm{C_{min}} = 0.1$ pF, $\mathrm{C_{step}} = 0.1$ pF, $\mathrm{C_{max}} = 10.0$ pF. The resulting far-field patterns are shown in Fig. 4. Note that the structure is six-fold symmetric and, therefore, only one sixth of the patterns and capacitances are reported here. The remaining

$$\boldsymbol{A} = \begin{bmatrix}
\left\{\mathrm{Re}\left(\frac{a_1Z_{11}}{a_1}\right) - \mathrm{Re}\left(\frac{a_1Z_{01}Z_{10}}{a_1Z_{00}}\right)\right\} & \left\{\mathrm{Re}\left(\frac{a_2Z_{12}}{a_1}\right) - \mathrm{Re}\left(\frac{a_2Z_{02}Z_{10}}{a_1Z_{00}}\right)\right\} & \left\{\mathrm{Re}\left(\frac{a_3Z_{13}}{a_1}\right) - \mathrm{Re}\left(\frac{a_3Z_{03}Z_{10}}{a_1Z_{00}}\right)\right\} & \cdots & \cdots & \left\{\mathrm{Re}\left(\frac{a_6Z_{16}}{a_1}\right) - \mathrm{Re}\left(\frac{a_6Z_{06}Z_{10}}{a_1Z_{00}}\right)\right\} \\
\left\{\mathrm{Re}\left(\frac{a_1Z_{21}}{a_2}\right) - \mathrm{Re}\left(\frac{a_1Z_{01}Z_{20}}{a_2Z_{00}}\right)\right\} & \left\{\mathrm{Re}\left(\frac{a_2Z_{22}}{a_2}\right) - \mathrm{Re}\left(\frac{a_2Z_{02}Z_{20}}{a_2Z_{00}}\right)\right\} & \ddots & & & \vdots \\
\left\{\mathrm{Re}\left(\frac{a_1Z_{31}}{a_3}\right) - \mathrm{Re}\left(\frac{a_1Z_{01}Z_{30}}{a_3Z_{00}}\right)\right\} & \left\{\mathrm{Re}\left(\frac{a_2Z_{32}}{a_3}\right) - \mathrm{Re}\left(\frac{a_2Z_{02}Z_{30}}{a_3Z_{00}}\right)\right\} & & & & \vdots \\
\left\{\mathrm{Re}\left(\frac{a_1Z_{41}}{a_4}\right) - \mathrm{Re}\left(\frac{a_1Z_{01}Z_{40}}{a_4Z_{00}}\right)\right\} & \left\{\mathrm{Re}\left(\frac{a_2Z_{42}}{a_4}\right) - \mathrm{Re}\left(\frac{a_2Z_{02}Z_{40}}{a_4Z_{00}}\right)\right\} & & & & \vdots \\
\left\{\mathrm{Re}\left(\frac{a_1Z_{51}}{a_5}\right) - \mathrm{Re}\left(\frac{a_1Z_{01}Z_{50}}{a_5Z_{00}}\right)\right\} & \left\{\mathrm{Re}\left(\frac{a_2Z_{52}}{a_5}\right) - \mathrm{Re}\left(\frac{a_2Z_{02}Z_{50}}{a_5Z_{00}}\right)\right\} & & & \ddots & \vdots \\
\left\{\mathrm{Re}\left(\frac{a_1Z_{61}}{a_6}\right) - \mathrm{Re}\left(\frac{a_1Z_{01}Z_{60}}{a_6Z_{00}}\right)\right\} & \left\{\mathrm{Re}\left(\frac{a_2Z_{62}}{a_6}\right) - \mathrm{Re}\left(\frac{a_2Z_{02}Z_{60}}{a_6Z_{00}}\right)\right\} & \cdots & & \cdots\ \cdots & \left\{\mathrm{Re}\left(\frac{a_6Z_{66}}{a_6}\right) - \mathrm{Re}\left(\frac{a_6Z_{06}Z_{60}}{a_6Z_{00}}\right)\right\}
\end{bmatrix} \tag{11}$$

TABLE I
NUMERICAL RESULTS FOR SIX PARASITIC ELEMENTS

Desired phi-direction	Max. Beam-direction	E_d/E_{max}	Directivity (dB)	Half-Power-Beam width
15°	15°	0.913	12.98	75°
30°	30°	0.928	12.37	77°
45°	45°	0.913	12.98	75°
60°	60°	1.000	13.95	68°

TABLE II
CAPACITANCES IN pF. DESIGN PARAMETERS SET TO: $C_{min} = 0.1$ pF, $C_{step} = 0.1$ pF, $C_{max} = 10.0$ pF. MONOPOLE 1 IS POSITIONED AT 60°; OTHERS FOLLOW AT 60° INTERVALS

Beam direction	C_1	C_2	C_3	C_4	C_5	C_6
15°	0.7	0.1	1.6	2.2	0.6	0.6
30°	0.6	0.4	1.5	1.5	0.4	0.6
45°	0.6	0.6	2.2	1.6	0.1	0.7
60°	0.7	0.7	0.1	1.6	0.1	0.7

6 elements (every 15°)

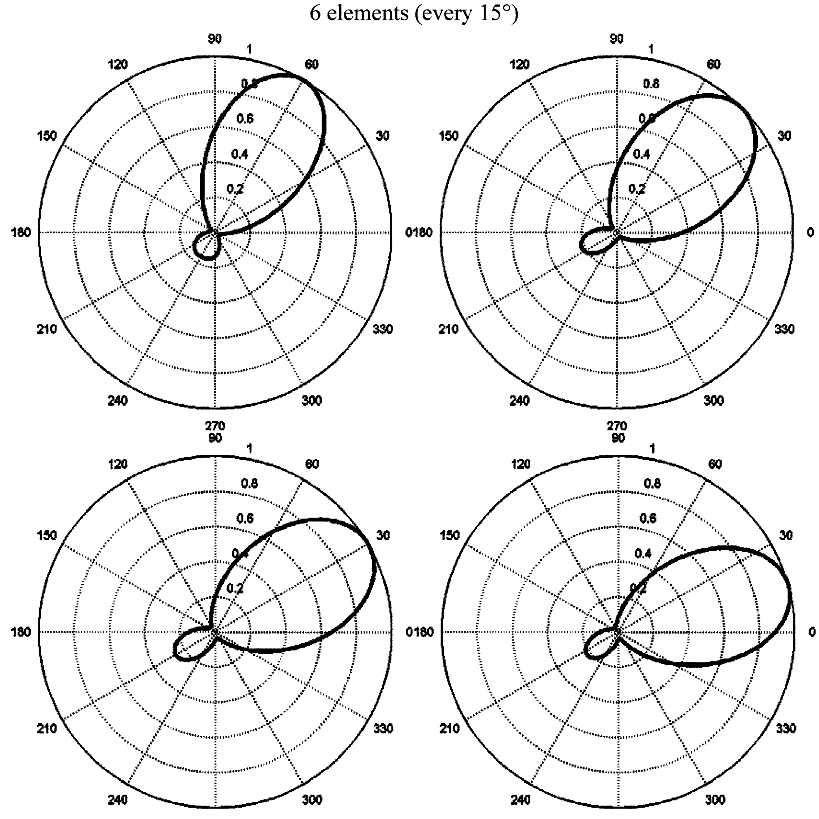

Fig. 4. Antenna patterns computed using six elements for beam pointing directions every 15°; e.g., in directions of 60°, 45°, 30°, and 15°.

sets follow straightforwardly from rotating patters and capacitances by increments of 60°. Note that the maximum side lobe level in Fig. 4 is −14 dB which shows very good beam compression.

Since the method is not restricted to a certain number of elements, we present some sample beam patterns for nine and twelve parasitic elements in Figs. 5 and 6, respectively. They have been calculated under the same restrictions for capacitance values as those in Table II. It is obvious that the beam pattern is not compromised by a higher number of elements and that the number of solutions with a maximum E-field increases with the number of elements. For all practical applications, though, six parasitic elements will suffice.

IV. CONCLUSION

The design of electronic beam steering arrays with parasitic elements is simplified through a straightforward calculation of the capacitances connected to the passive radiators. By solving separately for the amplitudes and phases of the currents in the parasitic elements, an analogue approach is obtained which reliably, and without any optimization, solves for a set of capacitances required to steer the beam in a specified direction. Moreover, the algorithm allows restraints to be set on the limits and accuracy of capacitance values which will ease requirements for practical implementations. It is demonstrated that the beamwidth and directivity are maintained (within small

9 elements (every 20°)

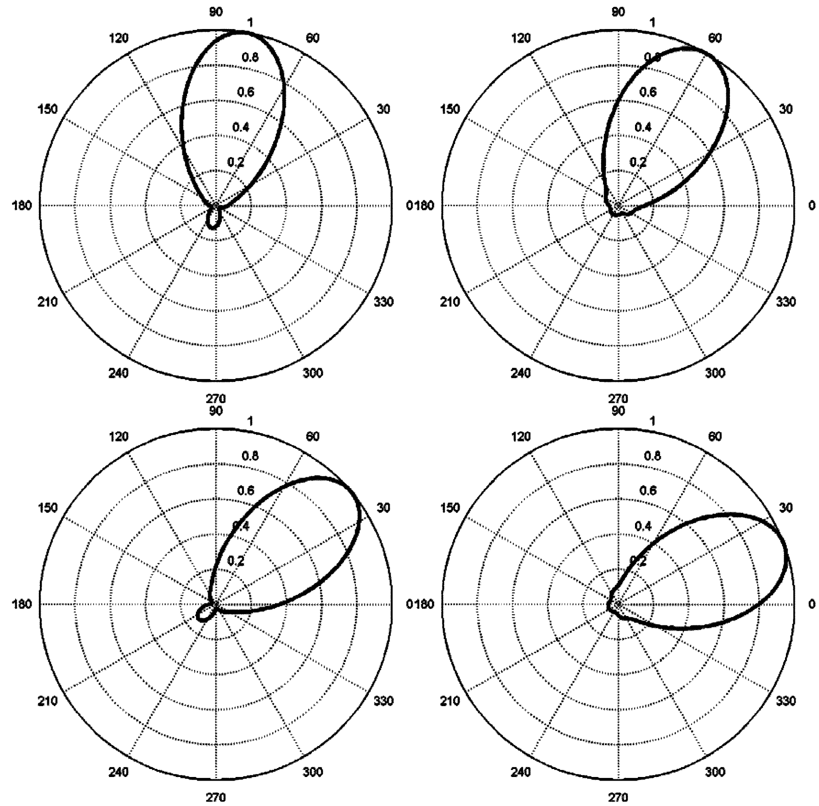

Fig. 5. Radiation patterns calculated using an array of 9 elements for beam pointing directions every 20°; e.g., in directions of 80°, 60°, 40°, and 20°.

12 elements (every 15°)

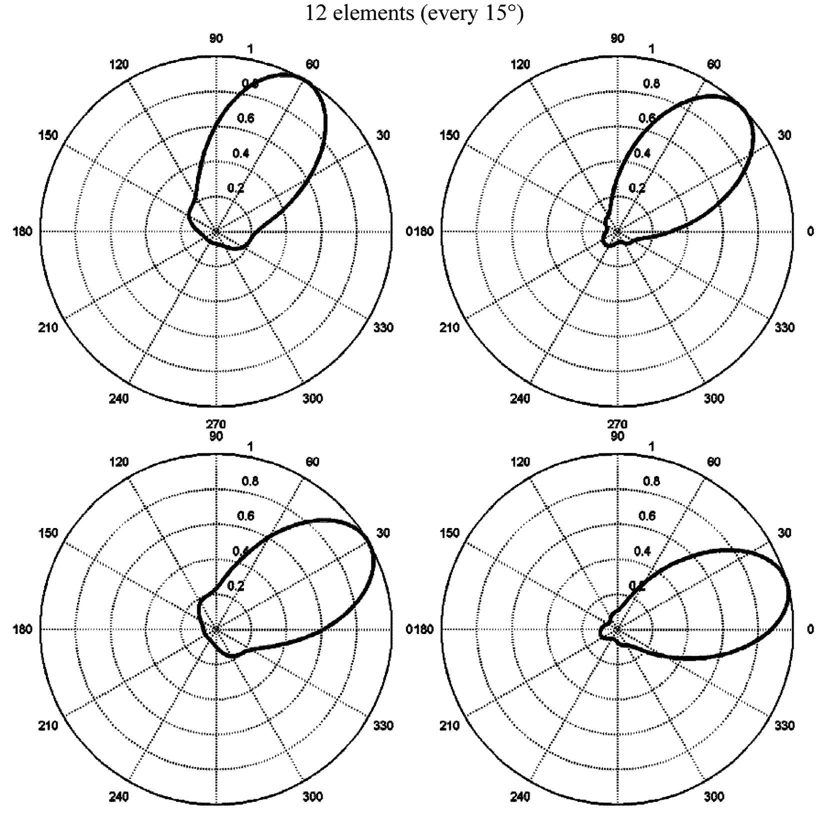

Fig. 6. Radiation patterns calculated using an array of 12 elements for beam pointing directions every 15°; e.g., in directions of 60°, 45°, 30°, and 15°.

margins) if the beam is rotated. Although the number is arbitrary, six parasitic radiators appear to be sufficient for wireless applications. Comparisons with NEC2 verify the pattern calculation.

REFERENCES

[1] G. J. Foschini and M. J. Gans, "On limits of wireless communications in a fading environment when using multiple antennas," *Wireless Personal Commun.*, vol. 6, pp. 311–335, Mar. 1998.

[2] J. Litva and T. Lo, *Digital Beamforming in Wireless Communications*. Boston, MA: Artech House, 1996, pp. 28–34.

[3] J. Butler and R. Lowe, "Beamforming matrix simplifies design of electronically scanned antennas," *Electron. Design*, vol. 9, pp. 170–173, April 1961.

[4] T. Ohira and K. Gyoda, "Hand-held microwave direction-of-arrival finder based on varactor-tuned analog aerial beamforming," in *Proc. Asia-Pacific Microwave Conf.*, Taipei, Taiwan, R.O.C., 2001, pp. 585–588.

[5] P. K. Varlamos and C. N. Capsalis, "Electronic beam steering using switched parasitic smart antenna arrays," *PIER*, vol. 36, pp. 101–119, 2002.

[6] C. A. Balanis, *Antenna Theory: Analysis and Design*. New York: Wiley, 1997.

Beat Schaer received the Dipl.-Ing. degree in electrical engineering from the Swiss Federal Institute of Technology (ETH) Zürich, Zürich, Switzerland, in 2003 and the M.B.E. in business and engineering in general management from the Steinbeis University Berlin, Germany, in cooperation with the European School of Business (ESB), Germany, the Indiana University, Terre Haute, and the University of Kitakyushu, Japan, in 2004.

From 2002 to 2003, he was a Junior Research Assistant at the University of Victoria, Victoria, BC, Canada, where he worked on analog beamforming with parasitic elements. In 2004, he was a Consulting Engineer in the area of microwave products with special focus on new product developments, feasibility studies and market strategy. He is currently a Project Engineer with the Swiss Broadcasting Corporation, Berne, Switzerland, working in the area of digital satellite and terrestrial television broadcast.

K. Rambabu received the Ph.D. degree from the University of Victoria, Victoria, BC, Canada, in 2004.

He has authored or coauthored 33 papers published in refereed journals and conferences. He holds a patent for beam shaping of a cellular base station antenna. His research interests include design and development of miniaturized passive microwave components and antennas for various applications.

Jens Bornemann (M'87–SM'90–F'02) received the Dipl.-Ing. and Dr.-Ing. degrees, both in electrical engineering, from the University of Bremen, Bremen, Germany, in 1980 and 1984, respectively.

From 1984 to 1985, he was a Consulting Engineer. In 1985, he joined the University of Bremen, as an Assistant Professor. Since April 1988, he has been with the Department of Electrical and Computer Engineering, University of Victoria, Victoria, BC, Canada, where he became a Professor in 1992. From 1992 to 1995, he was a Fellow of the British Columbia Advanced Systems Institute. In 1996, he was a Visiting Scientist at Spar Aerospace Ltd. (now EMS Technologies Incorporated), Ste-Anne-de-Bellevue, Québec, Canada, and a Visiting Professor at the Microwave Department, University of Ulm, Germany. From 1997 to 2002, he was a co-director of the Center for Advanced Materials and Related Technology (CAMTEC), University of Victoria. In 2003, he was a Visiting Professor at the Laboratory for Electromagnetic Fields and Microwave Electronics, ETH Zurich, Switzerland. He has coauthored *Waveguide Components for Antenna Feed Systems. Theory and Design* (Norwood, MA: Artech House, 1993) and has authored/coauthored more than 200 technical papers. His research activities include RF/wireless/microwave/millimeter-wave components and systems design, and field-theory-based modeling of integrated circuits, feed networks and radiating structures.

Dr. Bornemann is a Registered Professional Engineer in the Province of British Columbia, Canada. He serves on the Technical Program Committee of the IEEE MTT-S International Microwave Symposium and the editorial advisory board of the *International Journal of Numerical Modeling*. From 1999 to 2002, he served as an Associate Editor of the IEEE TRANSACTIONS ON MICROWAVE THEORY AND TECHNIQUES in the area of Microwave Modeling and CAD.

Rüdiger Vahldieck (M'85–SM'86–F'99) received the Dipl.-Ing. and Dr.-Ing. degrees in electrical engineering from the University of Bremen, Bremen, Germany, in 1980 and 1983, respectively.

From 1984 to 1986, he was a Postdoctoral Fellow with the University of Ottawa, Ottawa, ON, Canada. In 1986, he joined the Department of Electrical and Computer Engineering, University of Victoria, Victoria, BC, Canada, where he became a Full Professor in 1991. During fall 1992 and spring 1993, he was a Visiting Scientist with the Ferdinand-Braun-Institute für Hochfrequenztechnik, Berlin, Germany. In 1997, he accepted an appointment as a Professor of EM-field theory with the Swiss Federal Institute of Technology (ETH) Zürich, Zürich, Switzerland, and became Head of the Laboratory for Electromagnetic Fields and Microwave Electronics (IFH) in 2003. His research interests include computational electromagnetics in the general area of electromagnetic compatibility (EMC) and, in particular, for computer-aided design of microwave, millimeter-wave, and opto-electronic integrated circuits. Since 1981, he has authored or coauthored over 230 technical papers in books, journals, and conferences, mainly in the field of microwave computer-aided design.

Prof. Vahldieck is the past president of the IEEE 2000 International Zürich Seminar on Broad-band Communications (IZS'2000). Since 2003, he has been president and general chairman of the International Zürich Symposium on Electromagnetic Compatibility. He is a member of the Editorial Board of the IEEE TRANSACTIONS ON MICROWAVE THEORY AND TECHNIQUES. From 2000 to 2003, he was an associate editor for the IEEE MICROWAVE AND WIRELESS COMPONENTS LETTERS, and in January 2004, he became the editor-in-chief. Since 1992 he has served on the Technical Program Committee (TPC) of the IEEE MTT-S International Microwave Symposium (IMS), the IEEE MTT-S Technical Committee on Microwave Field Theory, and in 1999 and 2004 on the TPC of the European Microwave Conference. From 1998 to 2003, he was the chapter chairman of the IEEE Swiss Joint Chapter on Microwave Theory and Techniques, Antennas and Propagation, and EMC. Since 2005 he is the president of the Research Foundation for Mobile Communications, Switzerland. In 1996 he has received the J. K. Mitra Award of the Institution of Electronics and Telecommunication Engineers (IETE) for the best research paper in 1995 and he was the co-recipient of the Outstanding Publication Award of the Institution of Electronic and Radio Engineers in 1983.